ADVANCED ENERGY MATERIALS

Supporting Information

for *Adv. Energy Mater.*, DOI: 10.1002/aenm.201904118

Insights into the Storage Mechanism of Layered VS_2 Cathode in Alkali Metal-Ion Batteries

*Xiao Zhang, Qiu He, Xiaoming Xu, Tengfei Xiong, Zhitong Xiao, Jiashen Meng, Xuanpeng Wang, Lu Wu, Jinghui Chen, and Liqiang Mai**

Supporting Information

Insights into the Storage Mechanism of Layered VS_2 Cathode in Alkali Metal-ion Batteries

*Xiao Zhang, Qiu He, Xiaoming Xu, Tengfei Xiong, Zhitong Xiao, Jiashen Meng, Xuanpeng Wang, Lu Wu, Jinghui Chen, and Liqiang Mai**

X. Zhang, Q. He, X. Xu, Z. Xiao, J. Meng, L. Wu, J. Chen, Prof. L. Mai

School of Materials Science and Engineering

State Key Laboratory of Advanced Technology for Materials Synthesis and Processing

Wuhan University of Technology

Wuhan 430070, P. R. China

E-mail: mlq518@whut.edu.cn (Prof. L. Q. Mai)

T. Xiong

Department of Chemistry

City University of Hong Kong

Kowloon 999077, P. R. China

Dr. X. Wang

Department of Physical Science & Technology

School of Science

Wuhan University of Technology

Wuhan 430070, P. R. China

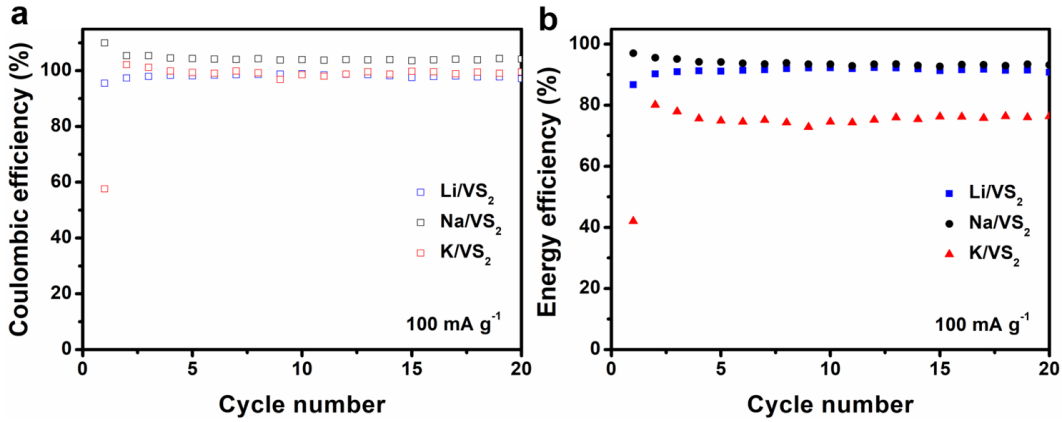

Figure S1. Coulombic efficiencies (a) and energy efficiencies (b) of VS_2 nanosheets at 100 mA g^{-1} in LIBs, SIBs, and PIBs, respectively.

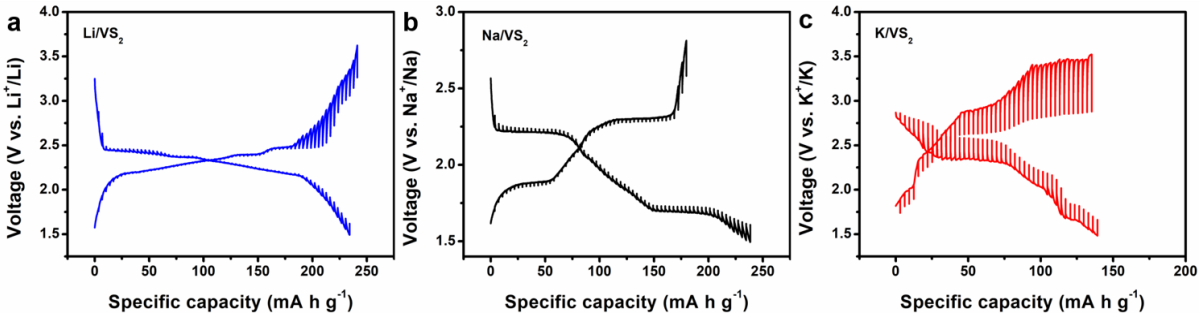

Figure S2. GITT curves of VS_2 nanosheets in LIBs (a), SIBs (b), and PIBs (c), respectively.

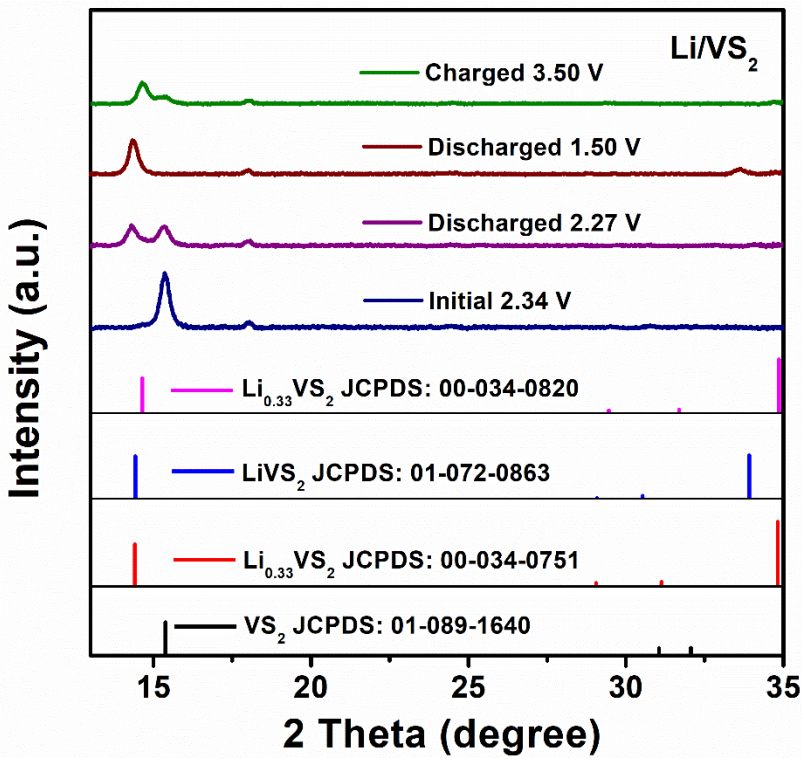

Figure S3. Selected *in-situ* XRD patterns during Li^+ insertion/extraction process.

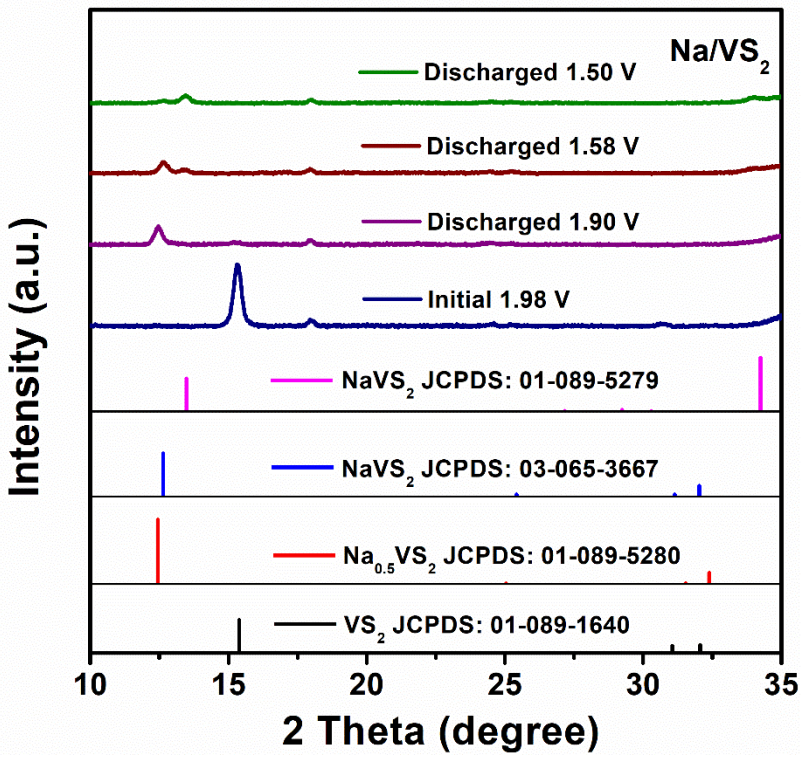

Figure S4. Selected *in-situ* XRD patterns during Na^+ insertion process.

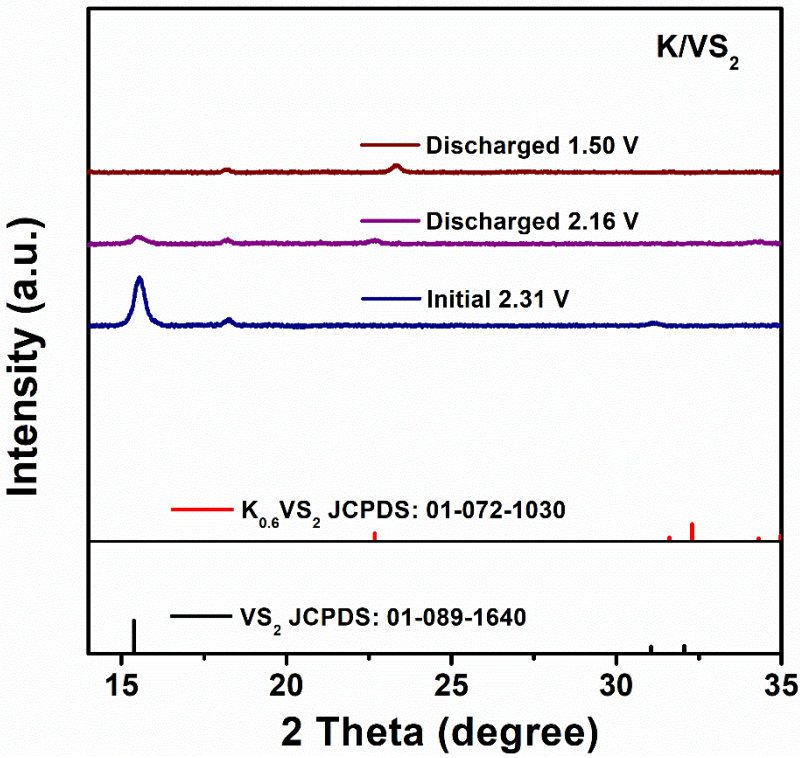

Figure S5. Selected *in-situ* XRD patterns during K^+ insertion process.

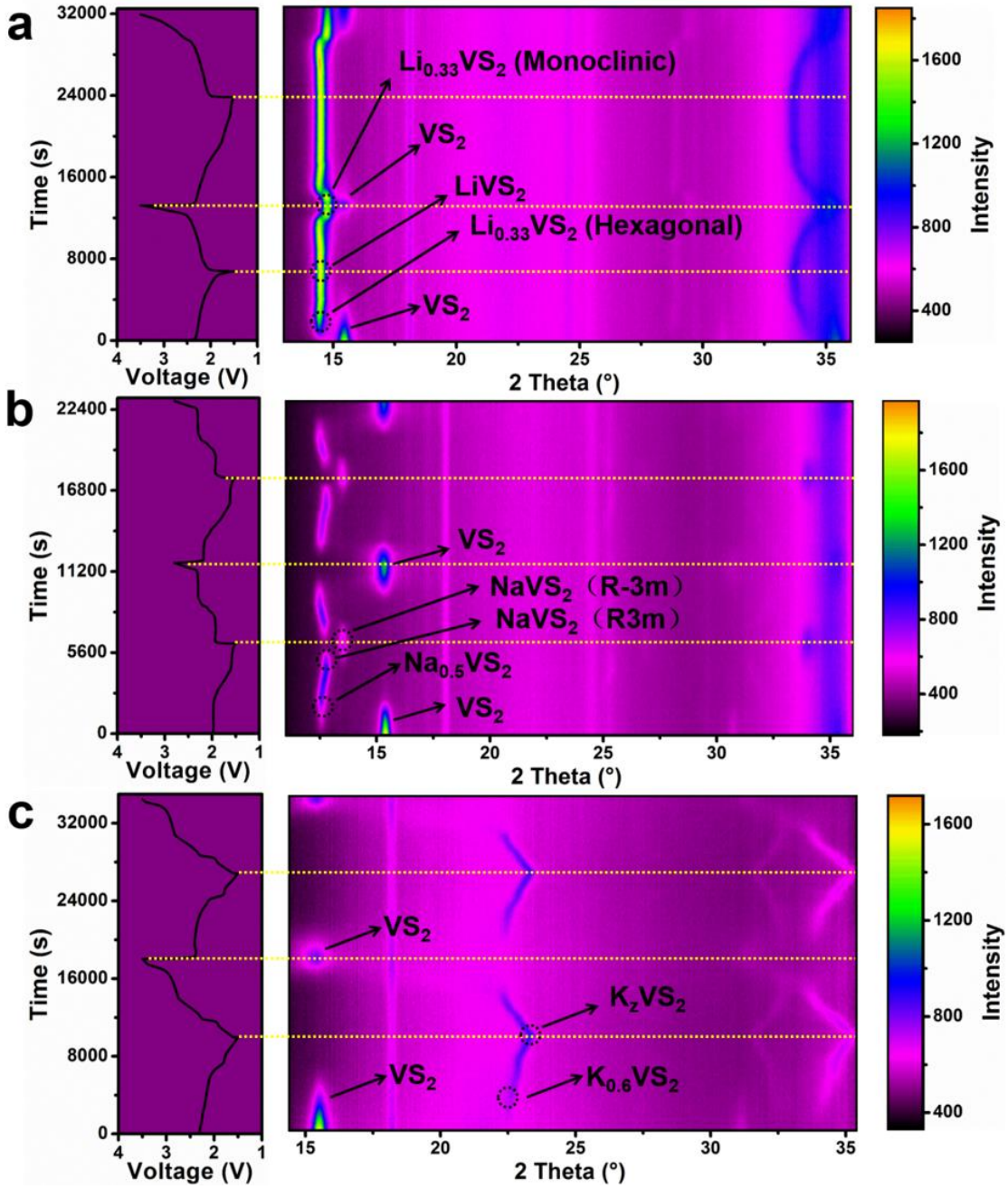

Figure S6. *In-situ* XRD patterns collected during the first two discharging/charging processes of VS_2 nanosheets from 13.0 to 36.0° in LIBs (a), from 11.0 to 36.0° in SIBs (b), and from 14.4 to 35.4° in PIBs (c), respectively.

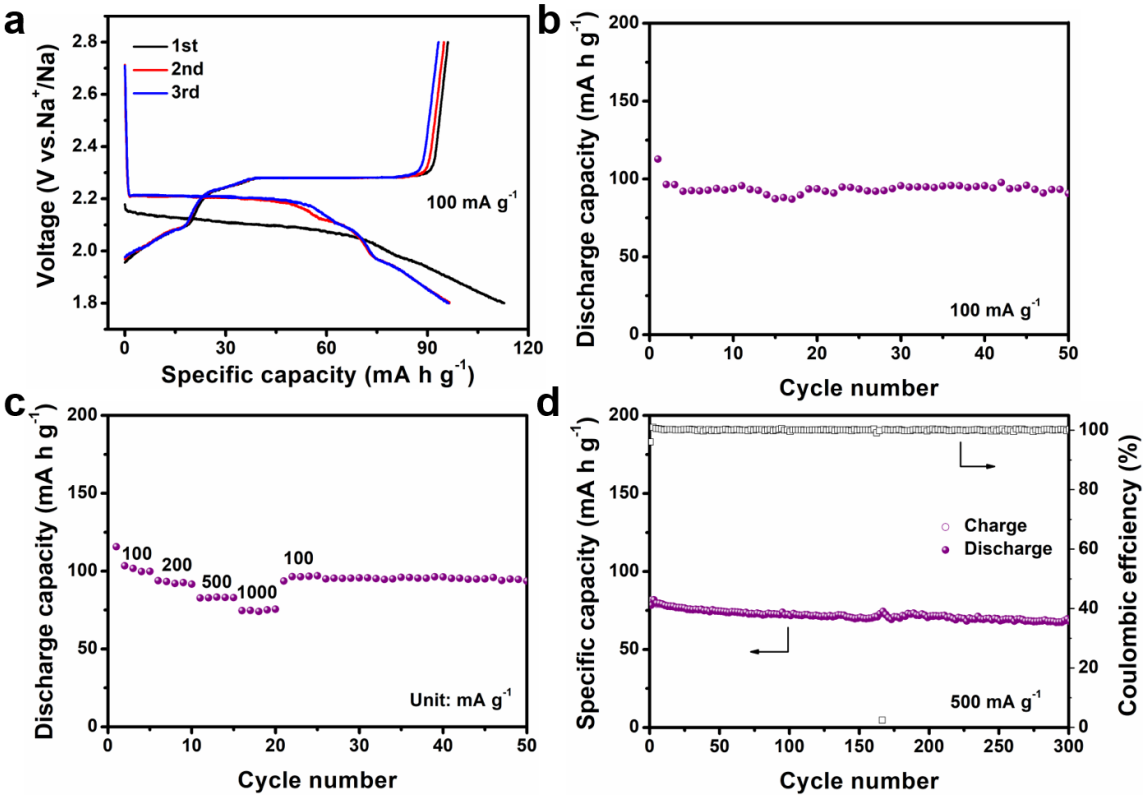

Figure S7. Galvanostatic discharge/charge profiles at 100 mA g^{-1} (a), cycling performance at 100 mA g^{-1} (b), rate capability (c), and long-term cycling performance at 500 mA g^{-1} (d) of VS_2 nanosheets in the voltage range of 1.8–2.8 V.

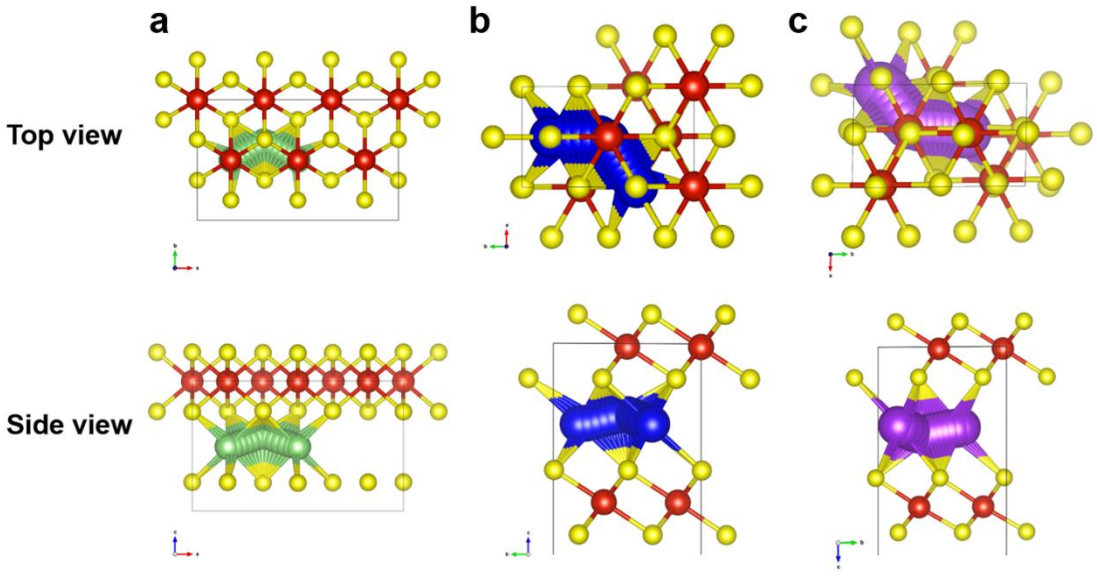

Figure S8. Schematic illustration of the migration paths for Li^+ (a), Na^+ (b), and K^+ (c) in VS_2 nanosheets.

Table S1. Crystal structure information of VS_2

	VS_2
Reference code	01-089-1640
Crystal system	Hexagonal
Space group	*P-3m1*
a	3.2210
b	3.2210
c	5.7550
Alpha (°)	90.0000
Beta (°)	90.0000
Gamma (°)	120.0000
Z	1.00

Table S2. Crystal structure information of Li_xVS_2

	$Li_{0.33}VS_2$	$LiVS_2$	$Li_{0.33}VS_2$
Reference code	00-034-0751	01-072-0863	00-034-0820
Crystal system	Hexagonal	Hexagonal	Monoclinic
Space group	*P-3m1*	*P-3m1*	*PE*
a	3.2770	3.3803	5.6590
b	3.2770	3.3803	3.2400
c	6.1520	6.1381	6.0500
Alpha (°)	90.0000	90.0000	90.0000
Beta (°)	90.0000	90.0000	91.0000
Gamma (°)	120.0000	120.0000	90.0000
Z	0.90	1.00	2.00

Table S3. Crystal structure information of Na_xVS_2

	$Na_{0.5}VS_2$	$NaVS_2$	$NaVS_2$
Reference code	01-089-5280	03-065-3667	01-089-5279
Crystal system	Rhombohedral	Rhombohedral	Rhombohedral
Space group	*R3m*	*R3m*	*R-3m*
a	3.3020	3.3460	3.5660
b	3.3020	3.3460	3.5660
c	21.3100	21.0200	19.6800
Alpha (°)	90.0000	90.0000	90.0000
Beta (°)	90.0000	90.0000	90.0000
Gamma (°)	120.0000	120.0000	120.0000
Z	3.00	3.00	3.00

Table S4. Crystal structure information of $K_{0.6}VS_2$

	$K_{0.6}VS_2$
Reference code	01-072-1030
Crystal system	Rhombohedral
Space group	*R3m*
a	3.2900
b	3.2900
c	23.5000
Alpha (°)	90.0000
Beta (°)	90.0000
Gamma (°)	120.0000

Table S5. A comparison of interlayer spacing between VS_2 and M_xVS_2 for the increment rate

	LIBs	**SIBs**	**PIBs**
d (The interlayer spacing of VS_2, Å)	5.755		
d (The interlayer spacing of	6.140	7.103 ($Na_{0.5}VS_2$)	7.833 ($K_{0.6}VS_2$)

M_xVS_2, Å)	($Li_{0.33}VS_2$, Hexagonal)		
The increment rate (%)	6.69	23.42	36.11